HHS Public Access

Author manuscript

Lab Chip. Author manuscript; available in PMC 2015 March 27.

Published in final edited form as:

Lab Chip. 2015 March 17; 15(7): 1638–1641. doi:10.1039/c5lc00055f.

Multicolored Silver Nanoparticles for Multiplexed Disease Diagnostics: Distinguishing Dengue, Yellow Fever, and Ebola Viruses

Chun-Wan Yen[a,b], **Helena de Puig**[c], **Justina Tam**[a,b], **José Gómez-Márquez**[d], **Irene Bosch**[a,b], **Kimberly Hamad-Schifferli**[c,e,*], and **Lee Gehrke**[a,f,*]

[a]Institute for Medical Engineering and Science, Massachusetts Institute of Technology Cambridge, MA USA 02139

[b]Winchester Engineering Analytical Center, Food and Drug Administration. Winchester MA USA 01890

[c]Dept. of Mechanical Engineering, Massachusetts Institute of Technology, Cambridge, MA 02139

[d]MIT Little Devices Lab and the MIT-SUTD International Design Centre

[e]MIT Lincoln Laboratory, Lexington MA 02420

[f]Dept. of Microbiology and Immunobiology, Harvard Medical School, Boston 02115

Abstract

Rapid point-of-care (POC) diagnostic devices are needed for field-forward screening of severe acute systemic febrile illnesses. Multiplexed rapid lateral flow diagnostics have the potential to distinguish among multiple pathogens, thereby facilitating diagnosis and improving patient care. Here, we present a platform for multiplexed pathogen detection using multi-colored silver nanoplates. This design requires no external excitation source and permits multiplexed analysis in a single channel, facilitating integration and manufacturing.

Lateral flow technology is well-suited to point-of-care (POC) disease diagnostics because it is robust and inexpensive, without requiring power, a cold chain for storage and transport, or specialized reagents. [1] Multiplexing, the detection of more than one marker in a single strip, offers further advantages for increasing speed and lowering costs by screening for multiple pathogens simultaneously.[2] While traditional lateral flow devices such as pregnancy tests screen for a single marker, recent technical advances permit multiplexing by spatial separation of lines on a single strip, or branched flow into separate test areas. [3-5] Potential disadvantages of multiplexing include non-specific binding and crossover, leading to false positive results. Here, we exploit the size-dependent optical properties of silver nanoparticles (Ag NPs) to construct a multiplexed lateral flow POC sensor. We conjugate triangular plate-shaped AgNPs of varying sizes to antibodies that bind to specific

*lgehrke@mit.edu. schiffer@mit.edu.

Electronic Supplementary Information (ESI) available: RGB analysis of test strips. See DOI: 10.1039/c000000x/

biomarkers, and thus use NP color to distinguish among three pathogens that cause a febrile illness. Because positive test lines can be imaged by eye or by using a mobile phone camera, the approach is adaptable to low-resource, widely deployable settings.

Noble metal NPs are attractive for lateral flow POC diagnostics because they are visible without an external excitation source or emission sensor, and unlike small-molecule dyes, resist photobleaching.[6-9] In addition, NP molar extinction coefficients typically exceed those of dyes by several orders of magnitude (10^8 vs. 10^4 $M^{-1}cm^{-1}$).[10] NP surface area is large and available for biofunctionalization with an antibody or nucleic acid aptamer that can bind to specific targets. More importantly, the colorimetric properties of NPs can be tuned by varying shape and/or size.[11] Triangular plate-shaped silver NPs (AgNPs) have narrow absorbances that are tunable through the visible spectrum,[12] resulting in easily distinguishable colors. AgNPs were synthesized using a seed-mediated growth method.[13] Growth of the yellow seeds to large AgNPs resulted in color changes from yellow to orange, red, blue, and green (Fig. 1a), with expected absorption spectrum shifts (Fig. 1b). Growth also resulted in a morphology change from spherical particles to triangular nanoplates (Fig. 1c-f). The AgNP colors are evident and distinguishable from one another when applied to paper and dried (Fig. 1g). TEM imaging (Fig. 1c-f) and dynamic light scattering (DLS, Fig. 1h, open symbols) confirmed that the NPs had distinct sizes, with mean diameters of D_{orange}= 30 ± 7 nm, D_{red} = 41 ± 6 nm, and D_{green} = 47 ± 8 nm (Fig. 1g).

AgNPs were prepared for lateral flow chromatography by conjugating antibodies to the NPs. Combining antibodies with AgNP in solution results in antibody binding to the AgNP mainly by electrostatic adsorption. Antibodies recognizing dengue virus (DENV) NS1 protein, Yellow Fever Virus (YFV) NS1 protein, and Ebola virus, Zaire strain (ZEBOV) glycoprotein GP were used. Ebola belongs to the *Filoviridae* virus family, while DENV and YFV are members of the *Flaviviridae* family. Our goal was to demonstrate detection without cross-contamination. We identified and characterized pairs of monoclonal antibodies directed against DENV NS1 (antibodies F4.24 and 8H7.G10, generated in our laboratory), YFV NS1 (antibody 9NS1, provided by Dr, Michael Diamond)[14] and well as ZEBOV glycoprotein (GP) (anti-ZEBOV antibodies, IBT Bioservices). Orange AgNPs, red AgNPs, and green AgNPs were conjugated with anti-YFV NS1 monoclonal antibody (mAb), anti-ZEBOV GP mAb, or anti-DENV NS1 mAb, respectively. After conjugation, AgNP surfaces were backfilled with thiolated PEG (mPEG-SH, MW=5,000) to enhance conjugate stability. Upon conjugation, the mean hydrodynamic size increased by ~50 nm (Fig. 1h), and the negative charge decreased (Fig. 1i), suggesting successful functionalization of the AgNPs with the antibodies.

As shown in the schematic (Fig. 2a), the components of a lateral flow chromatography assay include a sample pad (SP), conjugate pad (CP), nitrocellulose membrane (NC), and wick/absorbent pad. Each nitrocellulose fluidic pathway has four detection areas: a blank area to assess background binding to the NC, a second blank area that can be used to assess non-specific binding to an unrelated antibody, test area, and positive control area (bottom to top). The final component is the absorbent pad, which wicks fluid by capillary action. Conjugated AgNP-Ab were pipetted onto conjugate pads (CP) of the lateral flow assemblies, yielding orange, red, and green colors. The fourth CP (l-r, Fig. 2a) is brown because it was loaded

with a mixture of all three colored AgNPs. Complexes that yield a positive test result are shown schematically (Fig. 2b). A “sandwich” is formed when the viral protein ligand (NS1 or GP) is bound by both the antibody conjugated to the NP, and to the capture antibody loaded onto the test area of the nitrocellulose membrane. In a typical run, the sample solution containing the antigen (NS1 protein of DENV or YFV; GP of ZEBOV) is loaded into the sample pad. The liquid migrates through the CP, where the antigen binds to the AgNP-Ab. The AgNP-Ab/antigen complex then wicks through the strip by capillary action. As specific AgNP-Ab/antigen complexes flow through the strip, they are captured by the antibodies printed at the test line, creating a colored band at the test detection area. A positive control detection area is essential to demonstrate that the test ran completely and that the reagents were functional. We used positive control antibody that detects the Fc region of antibodies coupled to the NP. A colored test area is present at the positive control area due to the antibody on the AgNPs binding to an anti-immunoglobulin antibody loaded at the positive control detection area. Excess unbound AgNP-Ab flow into the absorbent pad.

A limit of detection analysis (LOD) for each of the three viral proteins is shown in Figure 2c-e. Antibody pairs (conjugated to the AgNP or loaded onto the test detection area) were specific to the YFV NS1 protein (orange, Fig. 2c), Ebola GP (red, Fig. 2d) or Dengue NS1 protein (green, Fig. 2e). The positive control detection area was loaded with anti-mouse immunoglobulin antibody to capture any mouse anti-human antibodies. Equal volumes of solutions containing the indicated protein concentrations were spiked into human serum (human male AB plasma purchased from Sigma Aldrich) loaded onto the sample pads (0-500 ng/ml). Positive signals at the positive control detection area confirmed that the test ran to completion and that AgNP-Ab were functional. In the absence of antigen, the test line was blank, indicating that AgNP-Ab-antigen binding is specific, and that non-specific adsorption of the AgNP-Ab to the test line was undetectable. LODs for YFV, DENV, and ZEBOV proteins were all in the range of 150 ng/mL. The maximal dengue NS1 serum concentration has been estimated to be 15-50 ug/ml[15, 16]. Therefore, our observed LOD is estimated to be 100-300X lower than this value, providing a significant window for early detection at lower serum NS1 concentrations. For DENV NS1, the LOD is more sensitive than the reported LOD of NS1 protein detected by the paper based lateral flow device.[17] The values for ZEBOV GP and YFV NS1 levels in human serum after infection have not been reported. Three independent measurements made from separate conjugation and antigen were repeated for LOD and the results are evaluated by ImageJ (Fig S1). RGB analysis using ImageJ further distinguished and characterized the AgNP (orange NPs: R =162 ± 15, G = 79 ± 10, B = 60 ± 4; red NPs: R = 219 ± 5, G = 101 ± 8, B = 151 ± 7; green NPs: R = 104 ± 13, G = 111 ± 15, B = 96 ± 14).

Multiplexed detection was explored using two different platforms. First, conjugate pads were prepared by loading with a mixture of orange, red, and green AgNPs conjugated with antibodies directed against YFV NS1 (orange), ZEBOV GP (red), and DENV NS1 (green), respectively (Fig. 3a). The second (“capture”) antibody directed against the viral protein was loaded separately onto individual detection areas of the fluidic paths. The sample pad of strip 1 was loaded with human serum only. The signal at each of the detection areas is undetectable, demonstrating very low background binding signal. When YFV NS1 (strip 2),

ZEBOV GP (strip 3) or DENV NS1 (strip 4) protein was applied to the sample pad, the orange, red, and green signals were observed only at the corresponding test detection area where the respective capture antibodies were loaded (strips 2-4). Again, background/non-specific binding at other test detection areas was minimal. When all three proteins were combined and applied to the sample pad (strip 5), orange, red, and green signals were observed at the position corresponding to the respective capture antibodies. The control detection area of each test was brown due to the presence of orange, red, and green AgNPs. RGB values of the control detection area indicated that all three colors of AgNPs were present (Supporting Information). The clear signal and low background/non-specific binding in each of the tests demonstrate effective multiplexed detection using mixtures of conjugated AgNPs with single capture antibodies loaded at the detection areas.

We next tested multiplexing by loading a single membrane detection area with a mixture of capture antibodies. The rationale of this approach is to reduce the number of test detection areas from three (Fig. 3a) to one (Fig. 3b). The three monoclonal capture antibodies were mixed at equimolar concentrations and then printed onto a single detection area on the test strip. Conjugate pads were again loaded with a mixture of the three AgNP-Ab conjugates. The predicted result of the experiment was that the single test detection area would be orange if YFV NS1 were present, red if ZEBOV GP were present, or green if DENV NS1 were present. Indeed, data are consistent with predicted results (Fig. 3b, strips 2-4). When all three proteins were mixed, the detection area was brown due to the mixture of orange, red, and green nanoparticles. RGB analysis was used to quantify the test line colors (Fig. S2 and S3), and the results showed that the values were similar to those of the individual AgNPs used in the lateral flow (Fig. 2c-e). The RGB value of each test is plotted in three axes (R, G, and B) (Fig. 3c). Each antigen detection forms an ellipse and none of ellipses overlap with the others, indicating that non-specific binding was not detected and that AgNP-Abs could bind without crossover reactivity. These data strongly suggest that multiplexed detection can be achieved in a single test line, which can facilitate miniaturization by increasing the number of targeted antigens in a given strip. This detection configuration could reduce test strip dimensions and simplify device design, potentially reducing material costs.

Conclusions

In summary, AgNP optical properties can be utilized for multiplexed POC diagnostics for infectious disease using their size-tunable absorption spectra. Distinguishing the color of the test lines can distinguish between different biomarkers, which can be achieved in a variety of formats including mobile phone apps.[18-20] LODs for the biomarkers of each disease were 150ng/mL. This type of design is ready for multiplexed detection with reduced device dimensions and cost.

Supplementary Material

Refer to Web version on PubMed Central for supplementary material.

Acknowledgement

Funding was from the NIH NIAID (AI100190). CWY and IB were supported by appointments to the Research Participation Program at the Winchester Engineering and Analytical Center, U.S. Food and Drug Administration, administered by the Oak Ridge Institute for Science and Education through an interagency agreement between the U.S. Department of Energy and FDA. JT is a Commissioner's Fellow of the U.S. Food and Drug administration. HdP was supported by the MIT/SUTD International Design Centre and a Rafael del Pino Fellowship. We thank CMSE at MIT for use of TEM imaging facilities, and Dr. Michael Diamond (Washington University School of Medicine) for providing antibody 9NS1.

References

1. Yetisen AK, Akram MS, Lowe CR. Lab Chip. 2013; 13:2210–2251. [PubMed: 23652632]
2. Geißler D, Ziessel RF, Butlin NG, Hildebrandt N. Angew. Chem. Int. Ed. 2010; 49:1396–1401.
3. Fenton EM, Mascarenas MR, López GP, Sibbett SS. ACS Appl. Mater. Interfaces. 2008; 1:124–129. [PubMed: 20355763]
4. Li, C.-z.; Vandenberg, K.; Prabhulkar, S.; Zhu, X.; Schneper, L.; Methee, K.; Rosser, CJ.; Almeide, E. 2011; 26:4342–4348.
5. Li Z, Wang Y, Wang J, Tang Z, Pounds JG, Lin Y. Anal. Chem. 2010; 82:7008–7014. [PubMed: 20704391]
6. Parolo C, Merkoçi A. Chem. Soc. Rev. 2013; 42:450–457. [PubMed: 23032871]
7. Hauck TS, Giri S, Gao Y, Chan WCW. Advanced Drug Delivery Reviews. 2010; 62:438–448. [PubMed: 19931580]
8. Nash MA, Waitumbi JN, Hoffman AS, Yager P, Stayton PS. ACS Nano. 2012; 6:6776–6785. [PubMed: 22804625]
9. Cordray MS, Amdahl M, Richards-Kortum RR. Analytical Biochemistry. 2012; 431:99–105. [PubMed: 23000603]
10. Huang X, Jain PK, El-Sayed IH, El-Sayed MA. Nanomedicine. 2007; 2:681–693. [PubMed: 17976030]
11. Mahmoud MA, O'Neil D, El-Sayed MA. Nano Letters. 2014; 14:743–748. [PubMed: 24328338]
12. Sherry LJ, Jin R, Mirkin CA, Schatz GC, Van Duyne RP. Nano Letters. 2006; 6:2060–2065. [PubMed: 16968025]
13. Homan KA, Souza M, Truby R, Luke GP, Green C, Vreeland E, Emelianov S. ACS Nano. 2011; 6:641–650. [PubMed: 22188516]
14. Chung NG, Thompson BS, Engle MJ, Marri A, Fremont DH, Diamond MS. Journal of Virology. 2006; 80:1340–1351. KM. [PubMed: 16415011]
15. Young PR, Hilditch PA, Bletchly C, Halloran W. Journal of Clinical Microbiology. 2000; 38:1053–1057. [PubMed: 10698995]
16. Alcon S, Talarmin A, Debruyne M, Falconar A, Deubel V, Flamand M. Journal of Clinical Microbiology. 2002; 40:376–381. [PubMed: 11825945]
17. Wang H-K, Tsai C-H, Chen K-H, Tang C-T, Leou J-S, Li P-C, Tang Y-L, Hsieh H-J, Wu H-C, Cheng C-M. Advanced Healthcare Materials. 2014; 3:187–196. [PubMed: 23843297]
18. Shen L, Hagen JA, Papautsky I. Lab on a Chip. 2012; 12:4240–4243. [PubMed: 22996728]
19. Vashist S, Mudanyali O, Schneider EM, Zengerle R, Ozcan A. Analytical and Bioanalytical Chemistry. 2014; 406:3263–3277. [PubMed: 24287630]
20. Zheng G, Patolsky F, Cui Y, Wang WU, Lieber CM. Nature Biotechnology. 2005; 23:1294–1301.

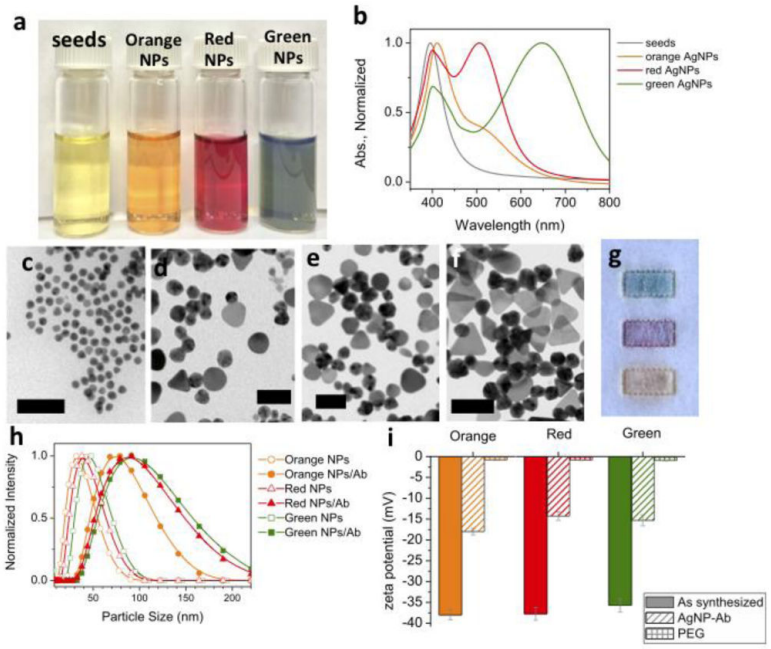

Fig. 1.

AgNPs for multiplexed detection. a) Vials of AgNPs during stepwise growth and b) their corresponding absorption spectra. TEM images of c) Ag seeds, d) orange AgNPs, e) red AgNPs, and f) green AgNPs. Scale bars: 50nm. g) Green, red, and orange (top to bottom) AgNPs on nitrocellulose paper. h) DLS and i) zeta-potential of AgNPs before and after mAb conjugation.

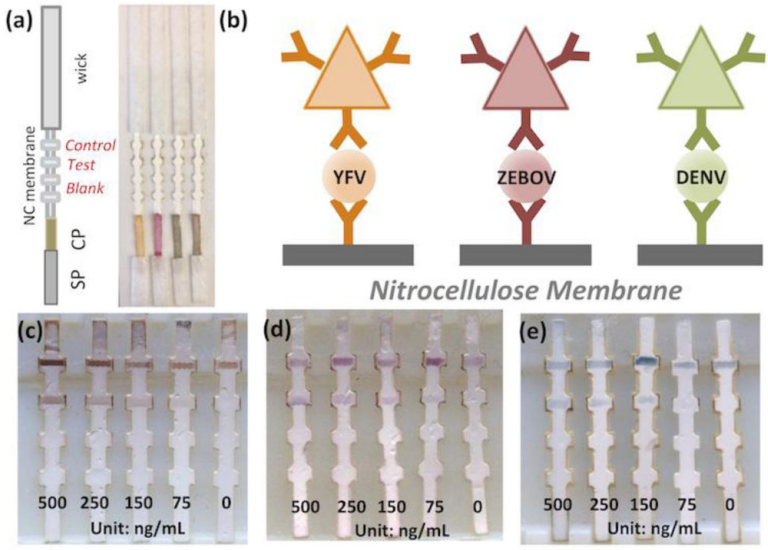

Fig. 2.

Individual testing of YFV, ZEBOV, and DENV using AgNPs. a) L-R, lateral flow strips with conjugate pads (CP) loaded individually with orange, red, and green AgNPs conjugated to mAbs (strips 1-3); the conjugate pad in strip 4 is loaded with a mixture of the three AgNP-Ab conjugates and is therefore brown in color. The NC strip is 20 mm X 3 mm. b) Schematic of the sandwich assay. AgNPs of each color are specific to a pathogen marker protein. Orange, red, and green AgNPs were conjugated with mAbs specific to YFV NS1, ZEBOV GP, and DENV NS1, respectively. (c)-(e) Limit of detection (LOD) of YFV NS1, ZEBOV GP, and DENV NS1 using the different AgNP-Abs. The YFV NS1, ZEBOV GP, and DENV NS1 antigen is purchased from the Native Antigen company, IBT Bioservices, and ProSpec, respectively. Test and control antibodies were printed in lines spaced by 2.5 mm using 50 nL droplets at a 0.5 mm pitch (Digilab MicroSys) at 2 mg/mL onto HiFlow Plus nitrocellulose membrane (240 s/cm flow rate; Millipore). The repeated LOD results are presented as Supporting Information (Fig S1).

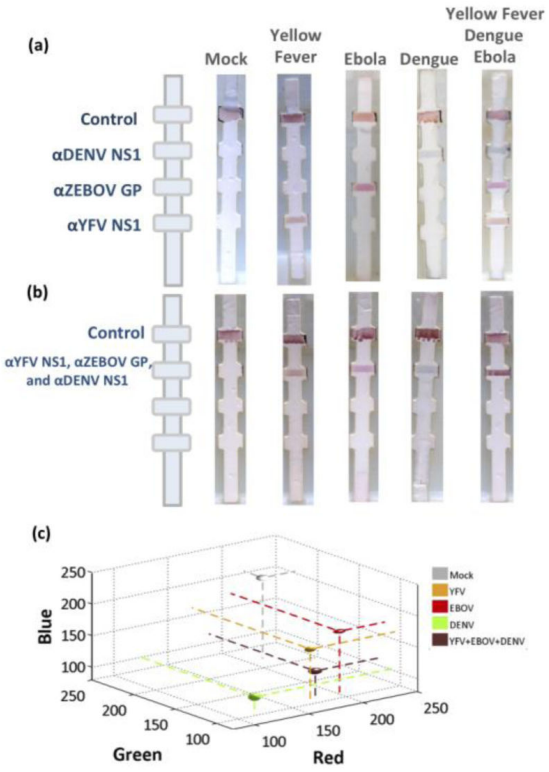

Fig. 3.

Multiplexed detection using AgNPs. a) Antibodies for viral proteins were printed on individual detection areas. A mixture of AgNP conjugated to anti-DENV NS1, anti-ZEBOV GP, and anti-YF NS1. When each of the infectious diseases is detected, the corresponding AgNPs forms a colored band at the specific line. b) Biomarkers are combined and printed into a single test line, which has a band of a different color depending on the antigen present: YFV: orange; EV: red; DV: green. The concentration of each antigen was 150 ng/mL. c) The RGB value of each antigen detection was plotted as an ellipse in 3D. The center of the ellipse is the mean RGB value and the length of the axes is the standard deviation. The standard deviations d calculated by Anova analysis on the order of 10^{-4} and that the differences between the test line relative to the control experiment (mock) are statistically significant. P values are <0.0005.